

Recent and episodic volcanic and glacial activity on Mars revealed by the High Resolution Stereo Camera

G. Neukum¹, R. Jaumann², H. Hoffmann², E. Hauber², J. W. Head³, A. T. Basilevsky^{1,4}, B. A. Ivanov^{1,5}, S. C. Werner¹, S. van Gassel¹, J. B. Murray⁶, T. McCord⁷ & The HRSC Co-Investigator Team*

¹Institut fuer Geologische Wissenschaften, Freie Universitaet Berlin, Malteserstrasse 74-100, Bldg D, 12249 Berlin, Germany

²DLR-Institut fuer Planetenforschung, Rutherfordstrasse 2, 12489 Berlin, Germany

³Department of Geological Sciences, Brown University, Providence, Rhode Island 02912, USA

⁴Vernadsky Institute of Geochemistry and Analytical Chemistry, RAS, Kosygin Street 19, 119991 Moscow, Russia

⁵Institute of Dynamics of Geospheres, Leninskiy Prospect 38, 119334 Moscow, Russia

⁶Department of Earth Sciences, Open University, Milton Keynes MK7 6AA, UK

⁷Hawaii Institute of Geophysics and Planetology, University of Hawaii, 2525 Correa Road, Honolulu, Hawaii 96822, USA

*A list of all members of the HRSC Co-Investigator team and their affiliations appears at the end of the paper.

The large-area coverage at a resolution of 10–20 metres per pixel in colour and three dimensions with the High Resolution Stereo Camera Experiment on the European Space Agency Mars Express Mission has made it possible to study the time-stratigraphic relationships of volcanic and glacial structures in unprecedented detail and give insight into the geological evolution of Mars. Here we show that calderas on five major volcanoes on Mars have undergone repeated activation and resurfacing during the last 20 per cent of martian history, with phases of activity as young as two million years, suggesting that the volcanoes are potentially still active today. Glacial deposits at the base of the Olympus Mons escarpment show evidence for repeated phases of activity as recently as about four million years ago. Morphological evidence is found that snow and ice deposition on the Olympus construct at elevations of more than 7,000 metres led to episodes of glacial activity at this height. Even now, water ice protected by an insulating layer of dust may be present at high altitudes on Olympus Mons.

On board the European Space Agency (ESA) Mars Express Orbiter, a multiple line scanner instrument, the High Resolution Stereo Camera (HRSC), is acquiring high-resolution colour and stereo images of the surface of Mars¹. Resolution down to 10 m per pixel coupled with large areal extent (swaths typically 60–100 km wide and thousands of kilometres long) means that small details can be placed in a much broader context than was previously possible. Among the major objectives of the experiment is an assessment of the level of recent geological activity on Mars, particularly the type of volcanic and climate-related deposits that might indicate areas of hydrothermal activity and recent water exchange conducive to exobiological activity.

We have used the new HRSC images and their particular qualities in mapping out terrain types for the interpretation of morphological features and topographic relationships from the three-dimensional data and high-resolution imagery, including the Super Resolution Channel (SRC) data (resolution down to 2.5 m per pixel)¹. The high-resolution colour data were very useful for distinguishing different materials. The combined use of the HRSC data and nested Mars Orbiter Camera (MOC) or SRC imagery has proven to be extraordinarily helpful in the interpretation of the morphologies and processes that shaped the landforms now visible. Here we focused on the time-stratigraphic relationships and the sequence of events to understand the geological evolution of the martian areas investigated. Time sequences were obtained by determining the number of superimposed impact craters and deriving absolute ages.

This approach has become a powerful tool of planetary studies since the early 1970s, when frequencies of craters per unit area of lunar basaltic lavas were compared with the absolute ages of these lavas determined through isotopic dating of the returned samples

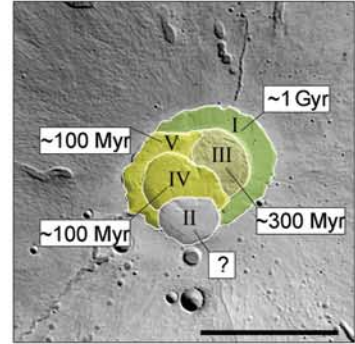
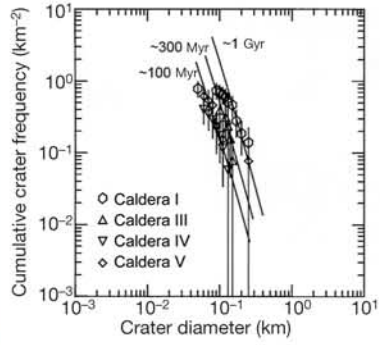
and have thus given us a reference scale for interplanetary comparison². These data, along with theoretical modelling and observational data of fluxes of crater-forming impactors for different parts of the Solar System, have made it possible to apply this method to different planets and satellites^{3–5}. For this study we used the recently updated cratering chronology model that combines the efforts of two major research groups in this area⁵.

The ages from crater counts are limited in accuracy almost exclusively by the statistical error³. Other error sources, such as undetected admixtures of secondary craters, volcanic or sublimation pits, are normally minor (<10% of the frequency of superposed craters)^{3,5}, provided the geological mapping of the areas and the counts are carried out by experienced observers. The statistical errors of individual data points in our counts are mostly <30% (one standard deviation, 1 σ). Because the whole distribution over a wider crater size range is used for fitting the theoretical size-frequency distribution to the measurements, the average statistical error of the data points over the ensemble of measurement is the proper measure for the uncertainty (which, in proportion to the number of data points, is much smaller), resulting in an average uncertainty of 20–30% in frequency. This translates into a 20–30% uncertainty in the absolute ages for ages younger than 3 gigayears (Gyr) and an uncertainty of only 100–200 million years (Myr) for ages older than 3 Gyr. Absolute ages may equally be affected by a possible systematic error of about a factor of two in the crater frequency for an assigned absolute age in the cratering chronology model used. This is due to an uncertainty in the underlying impact flux model used for Mars, relative to the lunar value^{4,5}.

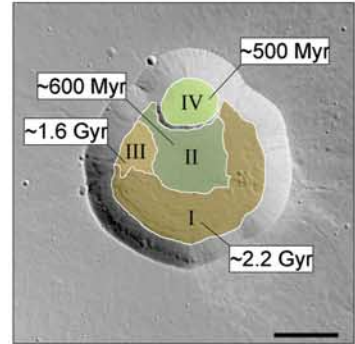
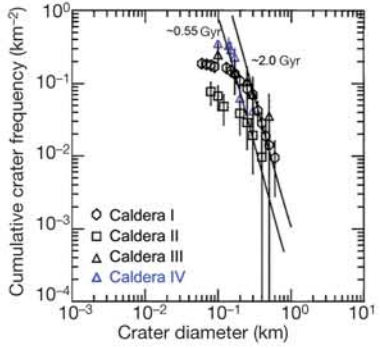
Time-stratigraphic relationships on martian volcanoes

The Tharsis region of Mars, a huge rise comprising almost 20% of

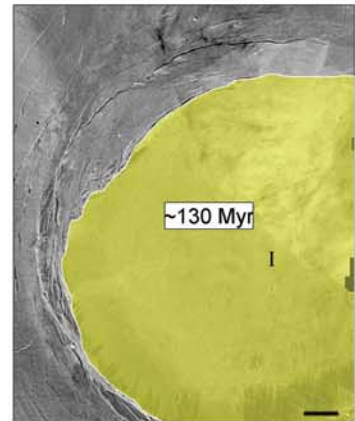
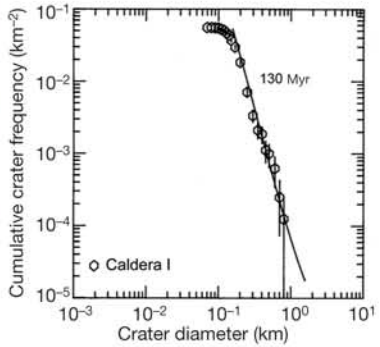
a Hecates Tholus



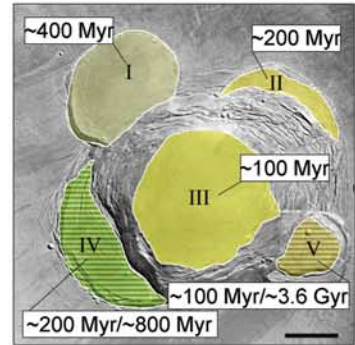
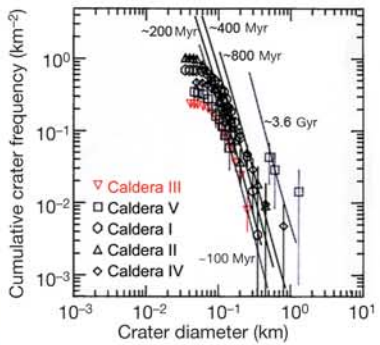
b Albor Tholus



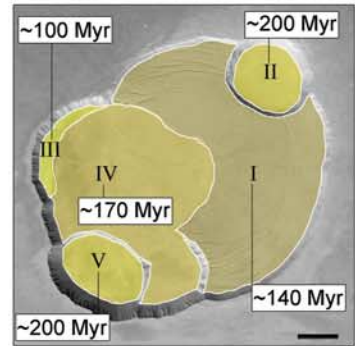
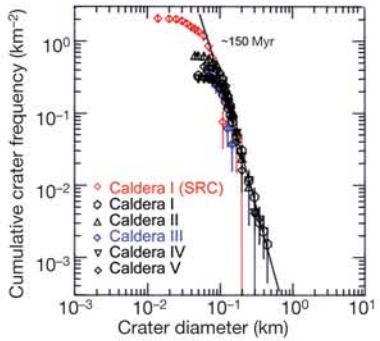
c Arsia Mons

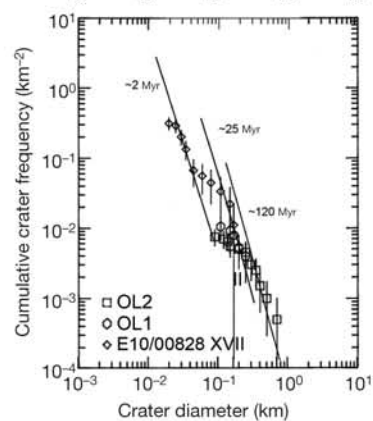
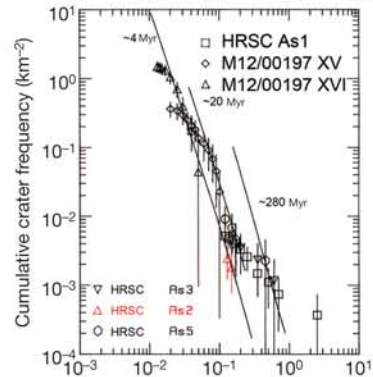
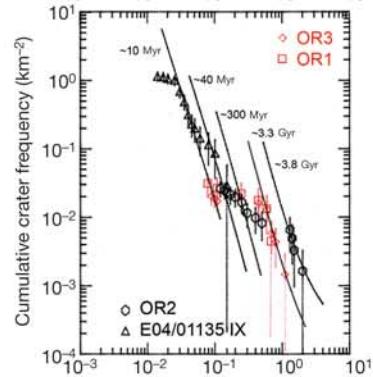
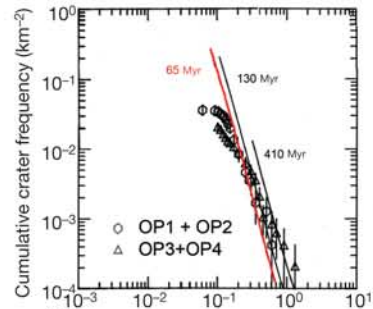
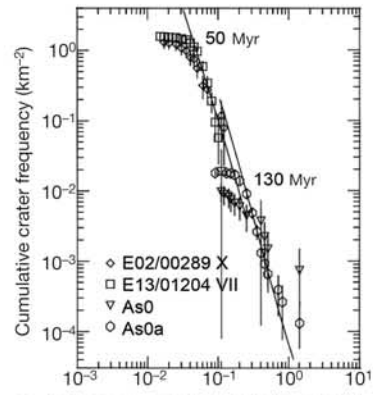
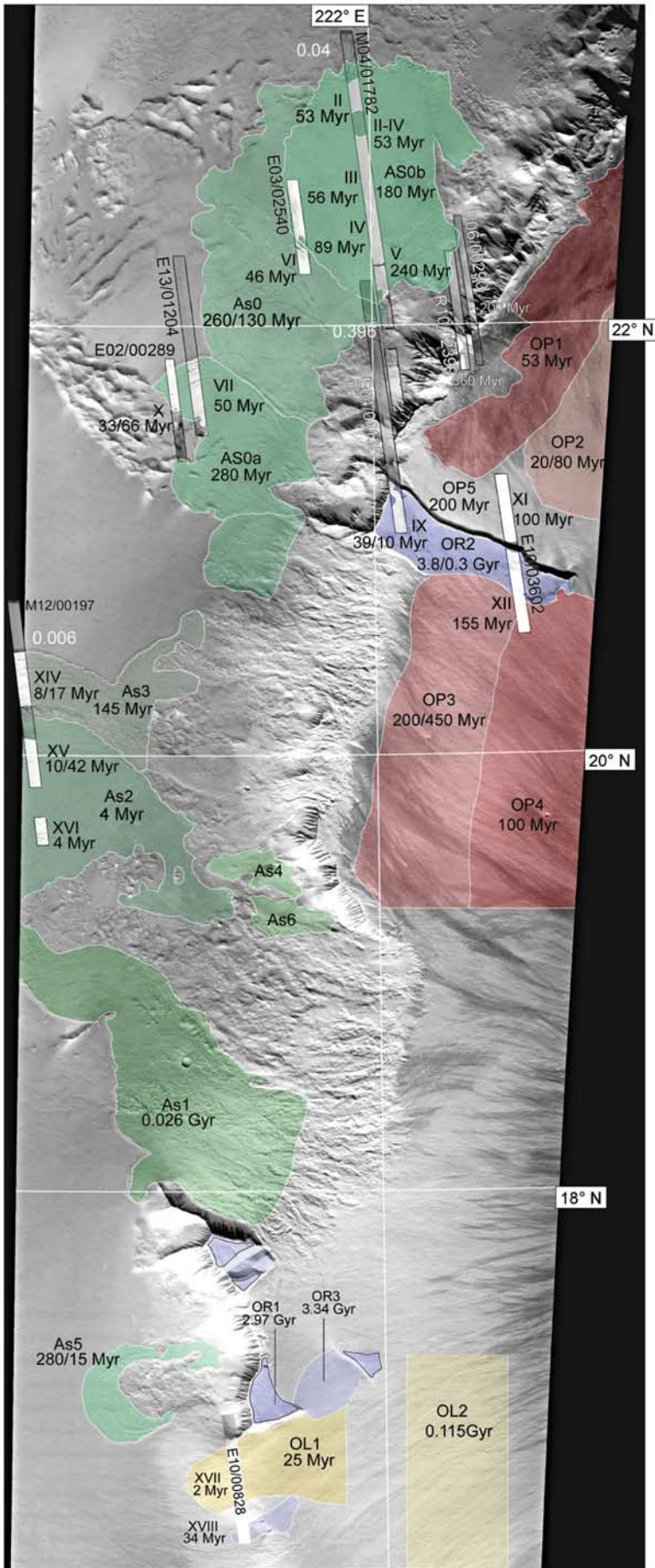


d Ascraeus Mons



e Olympus Mons





between caldera collapse events, suggesting that magma supply to major shield volcanoes on Mars must have been episodic, rather than continuous¹².

Olympus Mons, however, is unusual by comparison with other calderas. At least five arcuate caldera wall segments can be identified (Fig. 1e), but instead of being spread over hundreds of millions of years in age span, as observed at Ascraeus, Albor and Hecates, the ages of the five Olympus Mons caldera floors cluster in the period 100–200 Myr ago. Theoretically, the ages should be older for high-lying caldera floors and younger for the caldera floors at lower elevation. The different ages are very close to each other within the error limits of ± 50 Myr of the age measurements. Thus, the formation of all calderas could have happened in a narrow time span around 150 Myr ago.

It is obvious, however, from the imagery that some of the caldera floors were slightly resurfaced by subsequent thin lava flows or tectonic processes¹³ such as horst and graben formation, accompanied by mass wasting processes. Therefore, it is more likely that the calderas formed and were modified subsequently within a period of several tens of millions of years (equivalent to the differences in ages around the average age of 150 Myr). If the theoretical predictions¹² are correct, this implies that separate magma reservoirs were forming, solidifying, and re-forming on timescales averaging perhaps 20 Myr apart. Furthermore, the summit of Arsia Mons is dominated by a single huge caldera whose floor is dated at ~ 130 Myr ago—falling within the time span represented by the five Olympus Mons ages (~ 100 – 200 Myr ago).

These ages confirm some earlier measurements^{5,9} on the basis of MOC images in small areas of the calderas of Olympus Mons and Arsia Mons and indicate that the summits of these edifices were very active in essentially the geological present, the last 2–4% of Mars history. These ages provide supporting evidence for the repetitive and episodic nature of caldera formation, and thus magma supply, to the major shield volcanoes on Tharsis and Elysium (compare also with Hecates Tholus in Fig. 2). It is also an interesting coincidence that the summits of four of five of these edifices were very active 100–200 Myr ago, the period in which the crystallization ages of one of two major groups of martian basaltic meteorites fall¹⁴. This does not necessarily imply a genetic relationship but is a clue suggesting probably widespread volcanic activity on Mars at that time, generating large surface units that the basaltic meteorites may have come from.

It has long been known that the flanking rift zones of the Tharsis

Montes and lava flows cascading over the Olympus Mons scarp postdate much of the central edifice-building activity¹⁵. The new HRSC data permit more precise dating of the duration of activity in these regions. For example, on the lower flanks of Olympus Mons (Fig. 3) are observed flows for which crater size-frequency and age characteristics are interpreted to be representative of activity at ~ 115 Myr ago, ~ 25 Myr ago, and with HRSC and MOC data combined, as recently as 2.4 Myr ago.

Hydrothermal, fluvial, and glacial activity

Further evidence of very recent and episodic geological activity on Mars has been obtained by HRSC in the form of images and ages of several deposits related to recent climate change. We know that water in the form of ice exists at the polar caps and in the cryosphere of Mars¹⁶, and perhaps locally on the surface¹⁷. Only recently, however, has it become clear that the extreme variability of the obliquity of the spin axis of Mars and orbit eccentricity¹⁸ can cause significant mobilization of polar volatiles and their redeposition equatorward^{19,20}. Of particular interest are the types of deposits that are interpreted to represent the accumulation of water ice in non-polar regions, because these are very sensitive environmental indicators and have important implications for possible life and future automated and human exploration.

For these reasons, early targets for the HRSC instrument were parts of the Elysium region, and the western scarp of the Olympus Mons volcano. On the basis of Viking imagery, channels on the flanks of the Hecates shield have already been detected and interpreted as having been produced by running water^{21,22}. We have been able to study the Hecates shield at a resolution of 26 m per pixel in great detail and to determine the ages of some areas using crater-statistics methods (Fig. 2). MOC data were also used, as indicated in Fig. 2. The data show a wide age range over which volcanic activity and related mobilization of water (probably released hydrothermally or partly released through melting of snow caps by volcanically induced heating from underground) with subsequent glacial activity occurred. Here, we present only the gross time-stratigraphic relationships of the development in different areas on the volcano, starting more than 3.4 Gyr ago and shaping the volcano through different episodes of activity (for example, ~ 900 , 400 and 50 Myr ago) until very recent times of about 5 Myr ago. Fluvial and glacial activity can be recognized close to or in the depressions at the northwestern base of the volcano. In southern Elysium, to the southwest of Athabasca Valles, surface features have been observed on the HRSC imagery that look similar to pack-ice on Earth. The age of these deposits is only 5 Myr—in the same range as some of the glacial deposits on Olympus Mons and Hecates Tholus. Details of our findings are supplied elsewhere^{23,24}.

The other outstanding early target, the Olympus Mons volcano (Figs 3 and 4), is a site known to be characterized by lobate deposits thought to be of glacial origin¹⁷ and recently shown on the basis of the NASA Mars Global Surveyor (MGS) and Odyssey mission data to be a series of lobate rock-covered piedmont glaciers²⁵. These deposits are well illustrated in the new HRSC data (Fig. 4b). Therefore, it is now possible to determine more specific ages for them (Fig. 3 and Supplementary Table 1): 130 to 280 Myr for the major lobes, with some subunits in the 20–60 Myr range and locally as young as 4 Myr. These data indicate that the lobate deposits represent several phases of formation, most probably representing periods when significant snow and ice accumulation (possibly accompanied by hydrothermal mobilization of water that flowed down over the edge of the shield, entraining large amounts of non-icy surface material and then freezing) at the Olympus Mons scarp caused mobilization and flow of debris-covered piedmont glaciers into the surrounding low-lying regions.

In several places along the scarp, small linear tongue-like deposits can be seen to emerge from within the apparent accumulation zones of the larger lobate deposits (Fig. 4c). These are interpreted to be

◀ **Figure 3** Olympus Mons western scarp areas. HRSC-image base map with nested MOC data and depiction of the counting areas (left panel) and the resulting ages of the western near-escarpment area of the Olympus Mons volcanic shield, the 7-km-high escarpment and the adjacent plains area to the west with remnants of glacial features (five right panels). The counts show different episodes of resurfacing with erosion of craters and subsequent re-cratering. These episodes and processes are reflected in the different steepnesses of the distributions on the log–log plots, giving a kinked appearance. The flat parts show erosional effects; the steep parts show the re-cratering after the erosional episodes. The martian impact-crater size-frequency distribution^{12,13,14} has been fitted to the individual segments of the distribution, giving individual crater-frequency values for the different episodes; by application of the Hartmann–Neukum chronology¹⁴ individual absolute ages can be extracted. In this way it is possible to extract the evolutionary history of the area under investigation in detail. Here the fits to the crater frequencies partly have the character of average isochrons for a group of counts yielding similar numbers. Individual ages may be slightly different and are precisely given in Supplementary Table 1. The errors of the ages are usually around 20–30% for ages younger than 3 Gyr (only 100–200 Myr for older ages) owing to the statistical limitations. The error bars given represent a 1- σ error. In the same way, all ages of less than 2 Gyr may be affected by a possible systematic error of about a factor of two in the cratering chronology model¹⁴ used. North is at the top.

debris-covered alpine glaciers²⁶ that were previously undetected. Remarkably, the ages of these tongue-like deposits are so young that they cannot be reliably dated because of the lack of craters on them. These smaller tongue-like deposits are interpreted to have formed when conditions were sufficient to cause ice accumulation and local flow, but obviously did not form over the entire extended duration

represented by the underlying more widespread deposits. These very young tongue-like deposits are characterized by depressions at the base of the scarp and thus apparently lack an active accumulation zone, suggesting that they are relict features that are no longer forming today.

HRSC and local MOC data reveal evidence for sedimentary

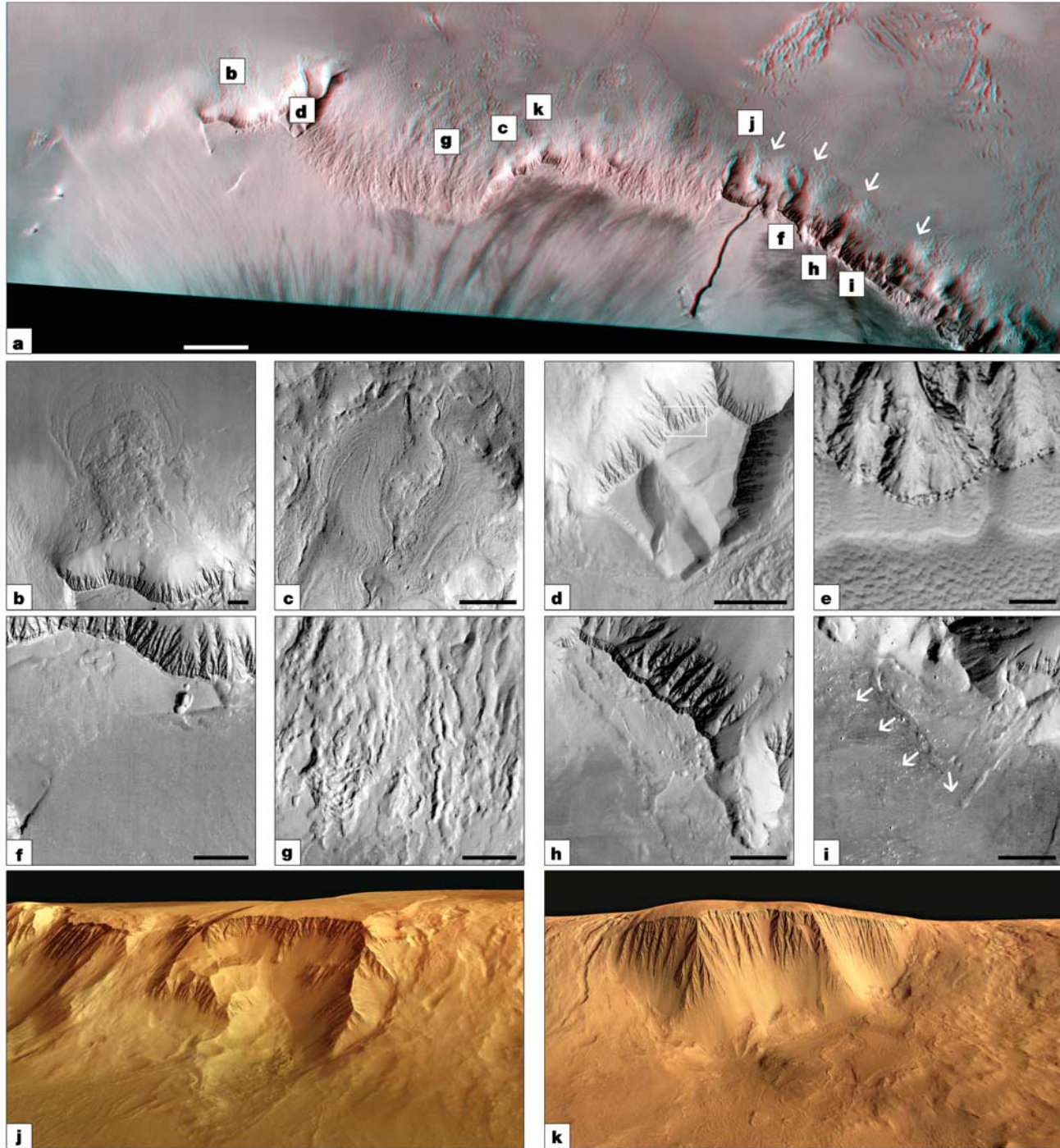


Figure 4 Ice–dust deposits and glaciers on Olympus Mons. **a**, Colour anaglyph for three-dimensional view of the region (scale bar, 30 km); labels b–k indicate designated areas shown on panels b–k (scale bar, 2 km). **b**, Glacier-type lobate flow. **c**, Tongue-like flows. **d**, Mesa at the scarp edge; small white square shows area of panel **e**. **e**, Part of MOC image E05-02498 showing fine layering in the upper part of the mesa material. **f**, Non-impact pits on mesa (upper right) and lava flows entering the mesa (centre left). **g**, Collapse-type depression and channel. **h**, The edge ridge with layers and the upper part of

U-shaped valley cut into the ridge and summit plateau. **i**, Glacier-type feature rimmed with small ridges (see arrows). **j**, **k**, Perspective views (from the west) of the western scarp of Olympus Mons showing steep ravined slopes and more gentle slopes with chaos-type depressions in their upper parts, as well as fluvial-type channels and glacier-like flows. The perspective view has been produced through a combination of HRSC nadir and colour image data and the DTM derived from the HRSC stereo data. North is to the right.

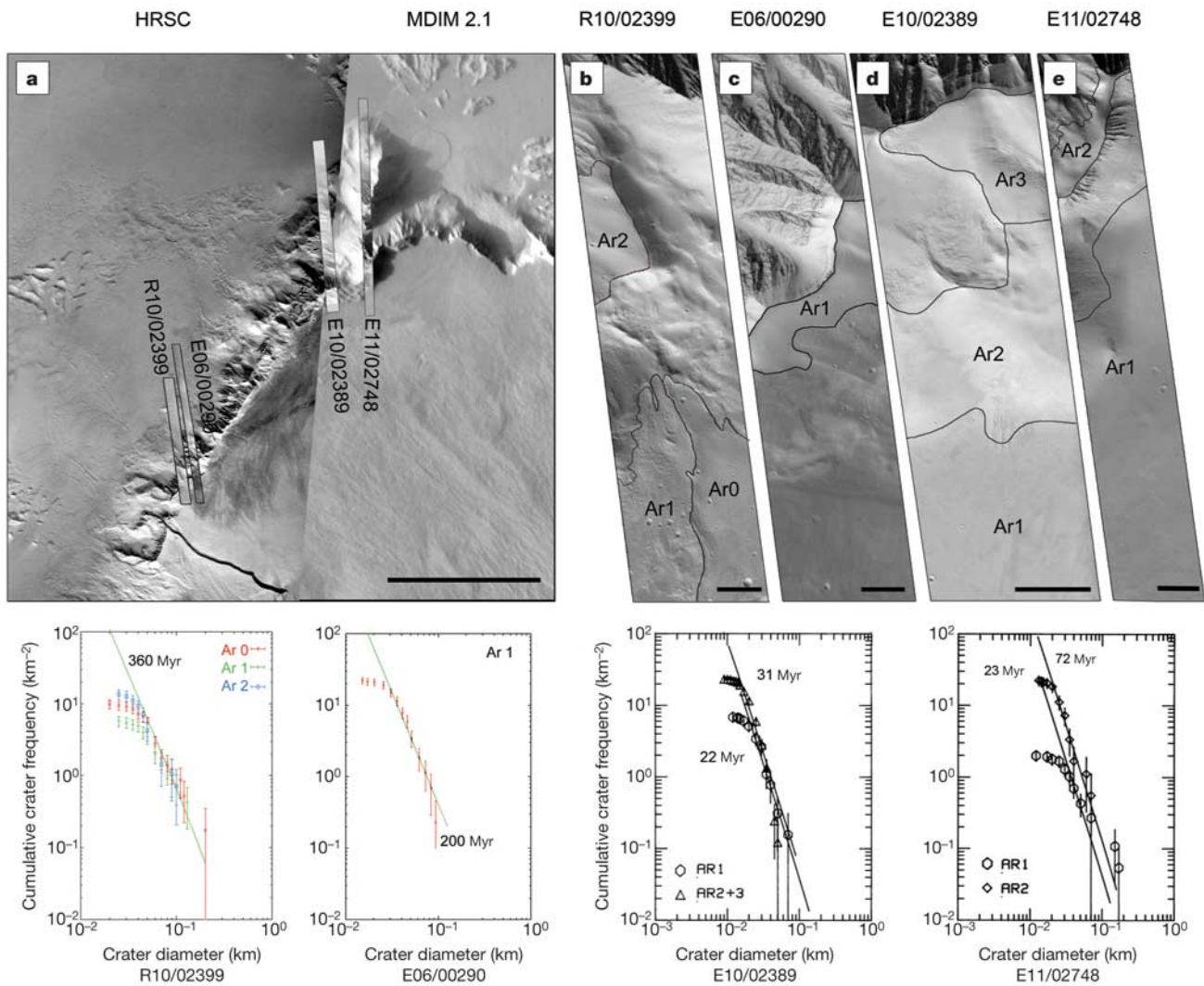


Figure 5 Base map (panels **a–e**) and crater statistics (four panels at bottom) of the areas on the northwestern part of Olympus Mons investigated for possible ice–dust coverage and age relationships. **a**, Mosaic of HRSC data (left) and Viking imagery (right) with the location of the MOC images used for morphological study and age determination; scale bar, 50 km. **b–e**, MOC images (scale bar, 1 km) with counting areas on flat terrain on the escarpment ridge with its ice–dust cover. **b**, Areas of measurement on MOC image R10/02399 and resulting ages derived from superposed crater frequencies. The ages are roughly the same for all three counting areas on the basis of the fit for intermediate-sized to large craters: 360 Myr with an uncertainty of about 70 Myr. Minor erosion of craters can be recognized in the subtle flattening of the measured distribution in comparison with the

fitted theoretical production function. The bending-over characteristics at the small-crater end here and in the other measurements in **c–e** stem from loss of craters at the resolution limit of the images. **c**, Areas of measurement on MOC image E06/00290 and resulting age of 200 ± 40 Myr. **d**, Areas of measurement on MOC image E10/02389 and resulting ages of 22 ± 4 Myr and 31 ± 6 Myr. The ages of the individual counting areas AR2 and AR3 have been determined separately with the same results (31 Myr). The AR1 measurements show that some erosion of the ice–dust cover seems to have taken place. **e**, Areas of measurement on MOC image E11/02748 and resulting ages of 23 ± 5 Myr and 72 ± 15 Myr. These ages correlate well with the ages (20 and 80 Myr) measured on adjacent lava flows (OP2 of the base map in Fig. 3). North is at the top. Error bars, $1-\sigma$ error.

deposits 50–100 m thick on the rim of the Olympus western scarp, sometimes in the form of mesas (Fig. 4d, e). These optically bright sediments show fine layering obviously different from that which could potentially be formed by accumulation of the lava flows typical of this volcano. We interpret these deposits to represent the remnants of accumulations of dust and ice high on the Olympus construct in previous geological periods. We believe that the presence on some mesas of rimless and deep sinkhole-type depressions (Fig. 4f, upper right) confirms this interpretation. In some places we also see that lava flowing upon these deposits causes their collapse (Fig. 4f, centre left).

Age measurements (Figs 3 and 4) show that the layers formed more than 300 Myr ago, possibly followed by further episodic activity or subsequent major erosional activity until about 65 Myr

ago, as seen on the escarpment ridge. Some data for the mesas, from the frequency of some large surviving craters that belong to the underlying substrate, yield age estimates that exceed 3 Gyr. That is close to earlier estimates of the age of the Olympus Aureole, interpreted to have formed by 3.4-Gyr-old gravitational slides of material from the western shield of the Olympus construct^{27,28}. This is an indication that the shield of Olympus Mons had already reached heights in excess of 7,000 m very early in its history. The eruption rates must have been very high at the beginning of the growth of the volcano.

Within the broad segments of the upper part of the scarp we observe depressions (Fig. 4g) that are morphologically similar to collapse depressions seen at the source areas of the outflow channels of Mars. The latter are believed to form as a result of release of large

amounts of water from below the surface, for example, the melting of ground ice by magma intrusion^{28,29}. Water (subsequently freezing to ice) seems to have been mobilized out of the ground hydrothermally. The collapse-type depressions of the Olympus scarp are also often accompanied by fluvial-type channels, although of relatively small size (Fig. 4h). We interpret these as having been formed by melting ice or ice-and-dust deposits via interaction with lavas.

Glaciers on the shield of Olympus Mons

The edge of the northern part of the scarp is rimmed by a ridge also covered with fine-layered deposits (Fig. 4j, k and Fig. 5a–e). The HRSC-based digital terrain model (DTM) model shows that the ridge stands 400–700 m above the surface adjacent to the east. We interpret the deposits on the ridge as a layer of ice and dust now protected from sublimation by a lag of dust. This ‘ice cap’ on the ridge formed about 400 Myr ago or earlier, as determined by measuring the superposed crater frequencies as given in Fig. 5. We identify different episodes of subsequent resurfacing of the ice cap at times of 200, 70 and 20–30 Myr ago. We have identified several valleys that are transverse to the ridge and cut into it. In a few cases, the valleys cut back into the summit plateau. The valleys have a U-shaped cross profile and end at the scarp foot with hummocky piles (arrows on Fig. 4a) often having lobate outlines. These are interpreted as debris-covered piedmont glaciers. These characteristics of the valleys suggest that glaciers ploughed them and that the source areas of those glaciers were high on the summit plateau. Moreover, in the potential source area of one of these valleys we see a lobate landform whose orientation suggests glacier movement to the east, towards the volcano centre (Fig. 4i). We estimate the age of this landform—now covered by dust, as are almost all other landforms of the region—to be 200–300 Myr (Figs 3 and 4j). We see evidence of sublimational or eolian degradation significantly erasing the cratering record, which implies that the lobate landform has not been active recently.

The colour data have been examined for effects of the presence of water ice, such as brightening of the surface and possibly flattening of the spectral slope. Colour ratio measurements were done for 16 major terrain types. Brightness in the four HRSC colour channels (centre wavelengths 440, 530, 750 and 970 nm) was calculated by applying the scaling factors from the ground calibration and additional factors derived from comparison with telescopic spectral data³⁰ and cross-calibration to data from the OMEGA experiment³¹. The measurements showed that the brightness values for each colour channel vary only within a factor of 1.5. All the measured ratios are close to those of ‘bright regions of Mars’³² indicating that all the studied terrains are dust-covered. If there is ice, then it appears to be covered and protected from sublimation by a sublimation lag of dust on top of the ice or ice–dust deposit.

The accumulation of ice necessary for developing the high-altitude glaciers and the dust–ice deposits on the mesas and the ridge could have happened at times of high inclination of the planet’s spin axis³³. Experimental data³⁴ and calculations³⁵ show that under current climate conditions sun-illuminated water ice (snow) sublimates quickly. But even a thin dust cover shifts the vapour pressure in the pore space to close to the saturation pressure and drastically decreases the sublimation rate of the buried ice³⁶. The buried ice (more probably an ice and dust mixture) may be practically stable (slowly sublimating) over millions of years, depending on the diffusive resistance of the upper dust cover against the vapour outflow to the dry atmosphere. Therefore, the layered deposits on the mesas and on the escarpment ridge, and the high-altitude lobate landform may still contain ice. This suggestion may be tested in the future by the MARSIS sounding radar³⁷ and OMEGA^{31,38} experiments on board Mars Express.

Conclusions

The new ages from the HRSC data: (1) confirm the very wide age range (billions of years) over which the Tharsis and Elysium regions were volcanically active; (2) reveal that summit caldera activity was periodic and often consistent with theoretical predictions of magma reservoir cooling and regeneration behaviour; (3) show that the most recent summit caldera activity on the Tharsis volcanoes was clustered ~100–200 Myr ago, practically coinciding with radiometric ages of several martian meteorites; (4) reveal that some of the youngest volcanism on the Tharsis edifices appears to be as young as several million years, thus suggesting that these volcanoes could well erupt in the future; (5) yield evidence for former hydrothermal mobilization of water at the western edge of the Olympus Mons volcano shield and probably on the Hecates Tholus volcano with subsequent development of glaciers; (6) reveal evidence for very young glaciations in the tropical regions of Mars; (7) reveal evidence for deposition of dust and ice and episodes of glaciation high on the Olympus Mons construct; and (8) suggest that water ice may now be present at high altitudes on the edge of the Olympus western scarp. □

Received 3 September; accepted 30 November 2004; doi:10.1038/nature03231.

1. Neukum, G., Jaumann, R. & the HRSC Co-Investigator and Experiment Team. *HRSC—The High Resolution Stereo Camera of Mars Express* 17–35 (European Space Agency Special Publication ESA SP-1240, 2004).
2. Malin, M. C. & Edgett, K. S. Mars Global Surveyor Mars Orbiter Camera: Interplanetary cruise through primary mission. *J. Geophys. Res.* **106**, 23429–23570 (2001).
3. Neukum, G., Ivanov, B. A. & Hartmann, W. K. Cratering record in the inner Solar System in relation to the lunar reference system. *Space Sci. Rev.* **96**, 55–86 (2001).
4. Ivanov, B. A. Mars/Moon cratering rate ratio estimates. *Space Sci. Rev.* **96**, 87–104 (2001).
5. Hartmann, W. K. & Neukum, G. Cratering chronology and the evolution of Mars. *Space Sci. Rev.* **96**, 165–194 (2001).
6. Neukum, G. & Hiller, K. Martian ages. *J. Geophys. Res.* **86**, 3097–3121 (1981).
7. Tanaka, K. The stratigraphy of Mars. *J. Geophys. Res.* **91**, E139–E158 (1986).
8. Greeley, R. & Spudis, P. D. Volcanism on Mars. *Rev. Geophys. Space Phys.* **19**, 13–41 (1981).
9. Hartmann, W. K. *et al.* Recent volcanism on Mars from crater counts. *Nature* **397**, 586–589 (1999).
10. Steinberger, B. Plumes in a convecting mantle: Models and observations for individual hotspots. *J. Geophys. Res.* **105**, 11127–11152 (2000).
11. Crumpler, L. C., Head, J. W. & Aubele, J. C. Calderas on Mars: Characteristics, structure and associated flank deformation. In *Volcano Instability on the Earth and Planets* (eds McGuire, W. J., Jones, A. P. & Neuberg, J.) *Geol. Soc. Spec. Pub.* **110**, 307–348 (1996).
12. Wilson, L., Scott, E. D. & Head, J. W. Evidence for episodicity in the magma supply to the large Tharsis volcanoes. *J. Geophys. Res.* **106**, 1423–1433 (2001).
13. Hauber, E. *et al.* The calderas on Mars—magmatic and tectonic characteristics as revealed through images of the High Resolution Stereo Camera (HRSC) on Mars Express. *Eur. Geophys. Union 1st Gen. Assembly* (abstr.) EGU04-A-07922 (2004).
14. Nyquist, L. E. *et al.* Ages and geologic histories of Martian meteorites. *Space Sci. Rev.* **96**, 105–164 (2001).
15. Crumpler, L. S. & Aubele, J. C. Structural evolution of Arsia Mons, Pavonis Mons and Ascraeus Mons: Tharsis region of Mars. *Icarus* **34**, 496–511 (1978).
16. Carr, M. *Water on Mars 229* (Oxford Univ. Press, New York, 1996).
17. Lucchitta, B. K. Mars and Earth: Comparison of cold climate features. *Icarus* **45**, 264–303 (1981).
18. Laskar, J. *et al.* Long term evolution and chaotic diffusion of the insolation quantities of Mars. *Icarus* **170**, 343–364 (2004).
19. Richardson, M. I. & Wilson, J. R. Investigation of the nature and stability of the Martian seasonal water cycle with a general circulation model. *J. Geophys. Res.* **107** doi:10.1029/2001JE001536 (2002).
20. Haberle, R. M., Murphy, J. R. & Schaeffer, J. Orbital change experiments with a Mars general circulation model. *Icarus* **162**, 66–89 (2003).
21. Mouginiis-Mark, P. J., Wilson, L. & Head, J. W. Explosive volcanism on Hecates Tholus, Mars: Investigation of eruption conditions. *J. Geophys. Res.* **87**, 9890–9904 (1982).
22. Gulick, V. C. & Baker, V. R. Origin and evolution of valleys on Martian volcanoes. *J. Geophys. Res.* **95**, 14325–14344 (1990).
23. Hauber, E. *et al.* Discovery of a flank caldera and very young and glacial activity at Hecates Tholus, Mars, in Mars Express HRSC images. *Nature* (submitted).
24. Murray, J. B. Evidence from the Mars Express High Resolution Stereo Camera for a frozen sea close to Mars’ equator. *Nature* (2004) (submitted).
25. Milkovich, S. M. & Head, J. W. Olympus Mons fan-shaped deposit morphology: Evidence for debris glaciers. *6th Int. Mars Conf.* (abstr.) 3149 (2003).
26. Head, J. W. *et al.* Recent ice ages on Mars. *Nature* **426**, 792–802 (2003).
27. Harris, S. A. The aureole of Olympus Mons. *J. Geophys. Res.* **82**, 3099–3107 (1977).
28. Lopes, R., Hiller, K., Neukum, G. & Guest, J. E. Further evidence of the Olympus Mons Aureole. *J. Geophys. Res.* **87**, 9917–9928 (1982).
29. Baker, V. R. *The Channels of Mars* (Austin Univ. of Texas Press, Austin, 1982).
30. McCord, T. *et al.* The color capabilities of the Mars Express High Resolution Stereo Camera. *Eur. Geophys. Union 1st Gen. Assembly* (abstr.) EGU04-A-06358 (2004).
31. Bibring, J.-P., *et al.* OMEGA: Observatoire pour la Mineralogie, l’Eau, les Glaces et l’Activite. 37–49 (European Space Agency Special Publication ESA SP-1240, 2004).
32. Banin, A., Clark, B. C. & Waenke, H. in *Mars* (eds Kiefer, H. H., Jakosky, B. M., Snyder, C. W. & Matthews, M. S.) 594–625 (Univ. Arizona Press, Tucson, 1992).

33. Head, J. W. *et al.* Recent mid-latitude glaciation on Mars: Evidence for snow and ice accumulation and flow in Mars Express HRSC data. *Nature* (in the press).
34. Kossacki, K. J., Komle, N. I., Leliwa-Kopystynski, J. & Kargel, G. Laboratory investigation of the evolution of cometary analogs: results and interpretation. *Icarus* **128**, 127–144 (1997).
35. Kossacki, K. J., Markiewicz, W. J., Skorov, Y. V. & Komle, N. I. Sublimation coefficient of water ice under simulated cometary-like conditions. *Planet. Space Sci.* **47**, 1521–1530 (1999).
36. Skorov, Y. V., Markiewicz, W. J., Basilevsky, A. T. & Keller, H. U. Stability of water ice under a porous nonvolatile layer: implications to the south polar layered deposits of Mars. *Planet. Space Sci.* **49**, 59–63 (2001).
37. Picardi, G., *et al.* *MARSIS: Mars Advanced Radar for Subsurface and Ionosphere Sounding*. 51–69 (European Space Agency Special Publication ESA SP-1240, 2004).
38. Bibring, J. P. *et al.* Perennial water ice identified in the south polar cap of Mars. *Nature* **428**, 627–630 (2004).

Supplementary Information accompanies the paper on www.nature.com/nature.

Acknowledgements We thank U. Wolf for help with the crater size-frequency distribution measurements and age evaluation, as well as W. Zuschneid and O. Fabel for their technical assistance and T. Denk for support in the colour data reduction effort. We also thank the ESTEC and ESOC staff, and the DLR Experiment and Operations team, especially T. Roatsch, K.-D. Matz, V. Mertens, J. Flohrer, E. Scholten, and K. Gwinner. J. Korteniemi, M. Aittola, P. Kostama and D. Williams helped with the image planning. This work forms part of the HRSC Experiment of the ESA Mars Express Mission and has been supported by the German Space Agency (DLR) on behalf of the German Federal Ministry of Education and Research (BMBF). Part of the data evaluation is supported by a grant from the German Science Foundation (DFG) within the scope of the priority programme ‘Mars and the Terrestrial Planets’.

Competing interests statement The authors declare that they have no competing financial interests.

Correspondence and requests for materials should be addressed to G. N. (gneukum@zedat.fu-berlin.de).

The HRSC Co-Investigator Team (Authors are arranged in alphabetical order) J. Alibert¹, A. T. Basilevsky², G. Bellucci³, J.-P. Bibring⁴, M. Buchroithner⁵, M. H. Carr⁶, E. Dorrer⁷, T. C. Duxbury⁸, H. Ebner⁹, B. H. Foing¹⁰, R. Greeley¹¹, E. Hauber¹², J. W. Head III¹³, C. Heipke¹⁴, H. Hoffmann¹², A. Inada^{15,18}, W.-H. Ip¹⁶, B. A. Ivanov¹⁷, R. Jaumann¹², H. U. Keller¹⁸, R. Kirk¹⁹, K. Kraus²⁰, P. Kronberg²¹, R. Kuzmin², Y. Langevin⁴, K. Lumme²², W. Markiewicz¹⁸, P. Masson²³, H. Mayer⁷, T. B. McCord²⁴, J.-P. Muller²⁵, J. B. Murray²⁶, F. M. Neubauer²⁷, G. Neukum (Principal Investigator)²⁸, J. Oberst¹², G. G. Ori²⁹, M. Pätzold²⁷, P. Pinet³⁰, R. Pischel¹², F. Poulet⁴, J. Raitala³¹, G. Schwarz³², T. Spohn¹² & S. W. Squyres³³

Affiliations for authors: 1, TU Berlin, D-10623 Germany; 2, Vernadsky Institute-RAS, Moscow 117975, Russia; 3, CNR/IFSI, 00133 Rome, Italy; 4, CNRS/IAS, 91405 Orsay cedex, France; 5, TU Dresden, D-01062 Germany; 6, USGS, MS 975 Menlo Park, California 94025, USA; 7, Universität der Bundeswehr München, D-85577 Neubiberg, Germany; 8, JPL, Pasadena, California 91109, USA; 9, TU München, D-80333 Germany; 10, ESTEC/SCI-SR, Postbus 299, NL-2200 AG Noordwijk, The Netherlands; 11, Arizona State University, Box 871404, Tempe, Arizona 85287-1404, USA; 12, DLR, D-12489 Berlin, Germany; 13, Brown University, Box 1846, Providence, Rhode Island 02912, USA; 14, Universität Hannover, D-30167 Germany; 15, Kobe University, 657-8501 Kobe, Japan; 16, National Central University (NCU), Chung-Li 320, Taiwan; 17, IDG-RAS, Moscow 117979, Russia; 18, MPAE, Postfach 20, D-37191 Katlenburg-Lindau, Germany; 19, USGS, Flagstaff, Arizona 86001, USA; 20, TU Wien, A-1040 Wien, Austria; 21, TU Clausthal, D-38678 Clausthal, Germany; 22, University of Helsinki, PO Box 14, SF-00014 Helsinki, Finland; 23, OrsayTerre, F-91405 Orsay Cedex, France; 24, PSI-Nw, Winthrop, Washington 98862, USA; 25, University College London WC1E 6BT, UK; 26, The Open University, Milton Keynes MK7 6AA, Buckinghamshire, UK; 27, Universität Köln, D-50923 Germany; 28, FU Berlin, D-12249, Germany; 29, IRSPS, I-65127 Pescara, Italy; 30, Observatoire de Midi-Pyrénées, F-31400 Toulouse, France; 31, University of Oulu, FIN-90401 Finland; 32, DLR, D-82234 Wessling, Germany; 33, Cornell University, Ithaca, New York 14853-1301, USA